Rosevear, P. R., Fox, T. L., & Mildvan, A. S. (1986) *Fed. Proc., Fed. Am. Soc. Exp. Biol. 45*, 1646.
Saenger, W. (1981) *Principles of Nucleic Acid Structure*, pp 51–104, Springer-Verlag, New York.
Sloan, D. L., & Mildvan, A. S. (1976) *J. Biol. Chem. 251*, 2412–2420.
Steinmetz, M. A., & Deal, W. C. (1966) *Biochemistry 5*, 1399–1405.
Stuart, D. I., Levine, M., Muirhead, H., & Stammers, D. K. (1979) *J. Mol. Biol. 134*, 109–142.
Tropp, J., & Redfield, A. G. (1981) *Biochemistry 20*, 2133–2140.
Wagner, G., & Wüthrich, K. (1979) *J. Magn. Reson. 33*, 675–680.
Yathindra, N., & Sundaralingam, M. (1973) *Biopolymers 12*, 297–314.

Structural Comparison of Acyl Carrier Protein in Acylated and Sulfhydryl Forms by Two-Dimensional ^{1}H NMR Spectroscopy†

Paul-James Jones, T. A. Holak, and J. H. Prestegard*
Department of Chemistry, Yale University, New Haven, Connecticut 06511
Received December 29, 1986

ABSTRACT: Sequence-specific assignments of ^{1}H NMR resonances are obtained for the backbone protons of *Escherichia coli* acyl carrier protein, acylated with an eight-carbon chain covalently attached to the prosthetic group thiol (octanoyl-ACP). Comparison of ^{1}H–^{1}H sequential connectivities in the NOESY spectra of octanoyl-ACP and the unacylated protein (ACPSH) indicates that secondary structure is largely conserved on acylation. Changes in resonance positions observed for certain groups of residues are interpreted in terms of a model that describes the spatial reorientation of secondary structural elements in the protein resulting from introduction of the acyl chain.

Acyl carrier proteins (ACPs)[1] are small, monomeric proteins that play an essential role in fatty acid biosynthesis for organisms with a type II fatty acid synthetase system. Although there is recent evidence for a more widespread function (Therisod et al., 1986), the accepted role of ACP is that of a shuttle, carrying the intermediates of fatty acid biosynthesis from site to site in the fatty acid synthetase system [for a review, see Vagelos (1973) and Volpe and Vagelos (1978)]. All ACPs studied are similar in that they are small (7.5–10 kDa), highly acidic proteins that have a 4'-phosphopantetheine prosthetic group. The intermediates of fatty acid biosynthesis are covalently attached to this group as acyl thio esters, and the prosthetic group is, in turn, covalently attached to the peptide backbone through a phosphodiester linkage to a serine side chain. Although the dominant view of ACP is that of a passive carrier, there is evidence to suggest that differences in the interaction of various acyl chains with a hypothetical binding site on ACP result in different enzyme affinities for these substrates and could be partly responsible for the fatty acid distribution produced by the synthetase system. For example, it is observed that thioesterase I is selective in the hydrolysis of palmitoyl- over *cis*-vaccenyl-ACPs, while it displays little selectivity when the corresponding acyl-CoAs serve as substrates (Barnes & Wakil, 1968; Spencer et al., 1978). Observations such as these have stimulated interest in the structural characterization of acyl-ACPs.

Among all known ACPs, the best characterized is that from *Escherichia coli*. This protein is quite representative of its class with 77 residues, with a large proportion (ca. 26%) of acidic residues, a much smaller proportion (ca. 8%) of basic residues, and a phosphopantetheine prosthetic group attached to Ser-36 (Majerus et al., 1965; Pugh & Wakil, 1965). The amino acid sequences of ACP from *E. coli* strains E-26 and K-12 are known (Vanaman et al., 1968a,b; S. Jackowski, J. E. Cronan, Jr., and C. O. Rock, personal communication). The sequence of strain B, the ACP used in this study, has been verified by NMR to be identical with that of strain E-26, with one exception, where Asp-24 is replaced by Asn (Holak & Prestegard, 1986). Although crystals yielding suitable diffraction data for ACP have been obtained (McRee et al., 1985), no crystal structure yet exists.

Recently, a secondary structural model for ACPSH has been proposed on the basis of interresidue contacts derived from analysis of two-dimensional nuclear Overhauser enhancement (NOE) data involving amide, α-, and β-protons (Holak & Prestegard, 1986). This structure agrees qualitatively with that previously proposed as the result of the application of the Chou–Fasman predictive algorithm (Rock & Cronan, 1979). Both proposals indicate a structure rich in α-helix, a conclusion further supported by earlier circular dichroism (Schulz, 1975) and optical rotary dispersion (Takagi & Tanford, 1968) studies. In the secondary structure de-

† This work was supported by a grant from the National Institutes of Health (GM 32243) and benefitted from instrumentation provided through shared instrumentation programs of the National Institute of General Medical Science (GM 32243S1) and the Division of Research Resources of NIH (RR02379).

[1] Abbreviations: ACP, acyl carrier protein; octanoyl-ACP, ACP with an eight-carbon acyl chain covalently attached to the prosthetic group thiol; ACPSH, ACP with a free prosthetic group thiol; RP-HPLC, reverse-phase high-pressure liquid chromatography; EDTA, ethylenediaminetetraacetic acid disodium salt; Tris, tris(hydroxymethyl)aminomethane; NMR, nuclear magnetic resonance; ppm, parts per million; NOE, nuclear Overhauser effect; COSY, two-dimensional J-correlated spectroscopy; relayed COSY, two-dimensional relayed coherence transfer spectroscopy; NOESY, two-dimensional NOE spectroscopy; d_{NN}, cross-relaxation connectivity between an amide proton and the amide proton on one of the neighboring residues; $d_{\alpha N}$, cross-relaxation connectivity between an amide proton and the α-proton of the preceding residue; $d_{\beta N}$, cross-relaxation connectivity between an amide proton and the β-proton(s) of the preceding residue.

0006-2960/87/0426-3493$01.50/0

termination by NMR, ACPSH was found to have four α-helices, which span residues 3–15, 37–51, 56–63, and 65–75 (Holak & Prestegard, 1986). Although a tertiary model for ACP has been proposed by our laboratory on the basis of a limited set of long-range interresidue NOE contacts (Mayo et al., 1983), this model is currently being revised with long-range distance constraints derived from NOESY data. One might expect the secondary and the forthcoming tertiary structure for ACPSH to be a good approximation of the structure of the acyl-ACPs. However, this is not certain, as studies by Rock and Cronan (1979) indicated that the presence of an acyl chain reduces the Stokes radius of ACP and renders it more resistant to pH-induced conformational change. One of our goals in this paper will be to compare secondary structure in ACPSH and an acyl-ACP.

It is reasonable to assume that any interaction between a fatty acid and ACP, or changes in the conformation of ACP, will manifest itself as proton chemical shift differences in the NMR spectra of ACPSH and the acyl-ACP. Many contributions to proton chemical shifts depend strongly on the presence and orientation of neighboring groups. Thus, while it may be difficult to interpret chemical shift changes quantitatively, qualitative aspects of structural differences should be reflected in chemical shift changes. Except in select cases, it is unlikely that changes in chemical shifts would be detected in the crowded one-dimensional proton NMR spectra typical of globular proteins. However, two-dimensional NMR techniques offer a convenient means of deconvoluting complex spectra, allowing one to detail minor changes in the spectra of related species. The combined use of COSY, relayed COSY, and NOESY spectra has been shown to be sufficient to allow the assignment of the majority of resonances for a number of small proteins, including ACPSH (Wagner & Wuthrich, 1982; Strop et al., 1983; Zuiderweg et al., 1983a; Ikura et al., 1985; Nehaus et al., 1985; Weber et al., 1985a,b; Holak & Prestegard, 1986; Klevit et al., 1986; Wemmer et al., 1986). In this paper, we plan to carry out a similar assignment for an acyl-ACP and compare the chemical shifts of selected resonances.

NOESY spectra contain additional information in that the cross-peaks observed correspond to physically proximate pairs of protons that are coupled by spin-spin relaxation. This has been exploited for the purpose of identification of secondary structural elements such as α-helices, β-sheets, and β-turns in a number of proteins (Strop et al., 1983; Zuiderweg et al., 1983b; Williamson et al., 1984; Weber, et al., 1985b; Holak & Prestegard, 1986; Klevit & Waygood, 1986; Wemmer et al., 1986). Since the intensity of NOESY cross-peaks exhibits a strong distance dependence, varying as the inverse sixth power of internuclear separation (Macura & Ernst, 1980), any changes in structure should be reflected in cross-peak intensity changes.

We have chosen for our analysis octanoyl-ACP. This was chosen as studies on acyl-ACPs (Rock & Garwin, 1979), suggest that most ACP–acyl chain interactions involve the first six to eight carbons of the acyl chain. As a result, octanoyl-ACP should exhibit most of the anticipated ACP-acyl chain interactions, yet it is a species that is conveniently prepared and purified. Thus, we believe that on comparison of octanoyl-ACP spectra with the corresponding ACPSH data a clearer picture of how the fatty acid interacts with the protein will emerge.

Materials and Methods

ACP was isolated from *Escherichia coli* B cells (Grain Processing, Muscatine, IA) according to the method of Rock and Cronan (1980) and was reduced to the free sulfhydryl form by the method of Cronan and Klages (1981). Octanoyl-ACP was prepared from ACPSH with *N*-octanoylimidazole, essentially as described by Cronan and Klages (1981).

Purification consisted of three steps, the first of which was passage through a Sephadex G-25 column to remove excess *N*-acylimidazole and other reagents. The column fractions corresponding to ACP were collected and were further purified by reverse-phase HPLC (RP-HPLC). The RP-HPLC was carried out at ambient temperature with a Vydac C-18 reverse-phase column (The Separations Group, Hesperia, CA) and a gradient elution with 2-propanol and 10 mM Tris–acetate, pH 6.5. The gradient consisted of a 10-min isocratic elution with 10% 2-propanol followed by a 10-min time period in which the amount of 2-propanol was linearly raised from 10% to 23%. All ACPs eluted in the subsequent 30-min time period, where the amount of 2-propanol was linearly increased from 23% to 30%. Under these conditions, octanoyl-ACP could be separated from all other ACP species. The final purification step consisted of loading the octanoyl-ACP onto a Sep-Pak C-18 cartridge (Waters, Milford, MA) and washing first with a solution containing 10 mM EDTA–10 mM KH_2PO_4, pH 7.5, and then with a solution containing 5 mM KH_2PO_4, pH 6.5. The octanoyl-ACP was eluted from the Sep-Pak with a solution of 50% 2-propanol–50% 5 mM KH_2PO_4, pH 6.5. After vacuum removal of the 2-propanol, the samples were freeze-dried and stored at −5 °C until needed.

Samples prepared in this manner proved sufficiently pure for NMR analysis as no spurious resonances, including those from ACPSH, were evident in one-dimensional ^1H NMR spectra. This purity is borne out in the analysis of relayed COSY data on octanoyl-ACP prepared in this manner. None of the cross-peaks assigned to minor species in the corresponding ACPSH preparations are evident, with the exception of a single cross-peak observed at $\omega_1 \sim 4.49$ ppm and $\omega_2 \sim 8.69$ ppm in ACPSH (Holak & Prestegard, 1986). The origin of this cross-peak is still unknown.

Samples for two-dimensional NMR analysis were typically in the range of 13–15 mM octanoyl-ACP and 35 mM KH_2PO_4, pH 6.3–6.5, and were freshly dissolved in either D_2O or H_2O/D_2O (4:1) prior to data acquisition. The reported pH measurements are uncorrected for isotope effects but are corrected from initial buffer pHs by comparing the chemical shift of the Ile-54 amide resonance with a calibration curve constructed from one-dimensional NMR titration studies.

^1H NMR spectra were acquired in the Fourier mode with quadrature detection on a home-built spectrometer operating at 11.5 T (490-MHz proton frequency). All spectra were acquired at 303 K, and chemical shifts are reported in parts per million (ppm) downfield from external sodium 4,4-dimethyl-4-silapentanesulfonate. For assignments, COSY (Aue et al., 1976; Wider et al., 1984), NOESY (Kumar et al., 1980; Wider et al., 1984), and relayed COSY (Eich et al., 1982; Bax & Drobny, 1985) experiments were performed. Typically, the two-dimensional spectra were acquired in absolute magnitude mode with 400–600 t_1 experiments, each containing 2K complex data points over a spectral width of 5.4 kHz in both dimensions. The carrier was placed on the water resonance, and in the case of the experiments performed in H_2O, the water resonance was irradiated with sufficient radio-frequency power to achieve saturation during all times except acquisition. Each t_1 data file contained 280–320 transients with a recycle time of 1.1 s, and two transients prior to acquisition of a t_1 data point were used to help achieve a steady state. Signal averaging times varied from 70 to 90 h. The relayed COSY

spectrum was acquired with a total mixing time of 50 ms, which was chosen to optimize magnetization transfers for valine, threonine, and isoleucine spin systems (Weber et al., 1985a). The NOESY spectra were acquired with mixing times of 80, 150, and 160 ms. For each of these experiments, the mixing time was randomly varied by 10% to eliminate coherent transfers. The data set acquired with the 160-ms mixing time afforded the best signal to noise ratio and was almost exclusively the basis for assignments. The other data sets were used to help determine the peaks in the 160-ms data set arising from spin diffusion.

After acquisition, the data was transferred to a VAX 11/750 computer equipped with a CSPI Minimap array processor. The data sets were typically multiplied by an unshifted sine bell function extending over 1024 complex t_2 points, followed by Fourier transformation. In the t_1 dimension, the data sets were zero-filled to 2K points, multiplied by a sine bell function usually extending 400–600 points, and then Fourier transformed. All the processing, display, and plotting software was written by Dr. Dennis Hare.

Reference ACPSH NMR data for chemical shift comparisons were obtained from a 10 mM sample of ACPSH in 55 mM KH_2PO_4, pH 5.6. While these sample conditions are somewhat different from those used for octanoyl-ACP, one-dimensional NMR titration studies indicate that with the exception of I54 the chemical shifts of the amide resonances of octanoyl-ACP show little change in the pH range 5.6–6.5.

Results

Assignment Strategy. In order to avoid bias in the assignment of octanoyl-ACP, the assignment process was carried out independently of that for ACPSH. The strategy used is essentially identical with that used for ACPSH, which utilized the methods described in detail by Wuthrich and co-workers (Wuthrich, 1983). This strategy consists of two phases. The first phase entails the identification of the various spin systems in the protein and assignment of those spin systems to amino acid types. This is achieved primarily by delineation of *J*-coupling patterns through the use of *J*-correlated spectra (COSY, relayed COSY). For certain amino acids (Gly, Ala, Thr, Ile, Val), the *J*-coupling patterns are unique enough so that an unambiguous assignment of these spin systems to an amino acid type is usually possible. For the other amino acids, a conditional identification of a spin system as belonging to a limited set of amino acids can often be made.

The second phase of the assignment process consists of the determination of the sequence-specific location of the amino acids assigned to previously identified spin systems. This is achieved primarily through the information supplied about sequential amino acids from NOESY spectra. Previous studies (Billeter et al., 1982; Wagner & Wuthrich, 1982) have indicated that most of the cross-peaks seen in NOESY spectra arise as the result of intraresidue connectivities, or connectivities involving sequentially adjacent residues. The connectivities involving sequentially adjacent residues fall primarily into three categories: amide–amide [NH(i)–NH($i \pm 1$)], amide–α [NH(i)–H$_\alpha$($i-1$)], and amide–β [NH(i)–H$_\beta$($i-1$)] connectivities. These are often referred to as d_{NN}, $d_{\alpha N}$, and $d_{\beta N}$ connectivities, respectively. This information is used to link amino acids together until a grouping unique to a specific location in the sequence is found.

The type of interresidue cross-peaks observed in NOESY spectra can depend on the local secondary structure. In proteins with a high α-helical content, stretches of strong, easily resolved d_{NN} cross-peaks are observed, with moderately strong $d_{\beta N}$ and weaker $d_{\alpha N}$ cross-peaks evident (Billeter et al., 1982; Wuthrich et al., 1984). Since ACP has a high α-helical content, the obvious sequential assignment strategy is to use d_{NN} cross-peaks to connect residues together, relying on the $d_{\beta N}$ and $d_{\alpha N}$ cross-peaks to confirm our assignments and to circumvent areas where the d_{NN} cross-peaks are missing, or are obscured by spectral overlap.

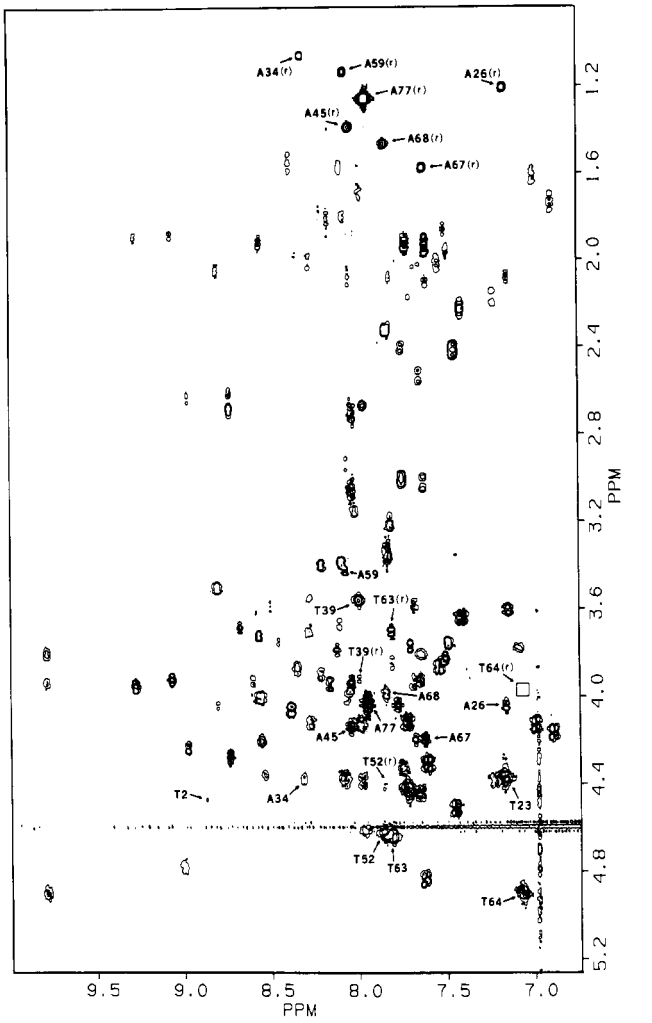

FIGURE 1: Portion of a relayed COSY spectrum showing the NH–H$_\alpha$ fingerprint and NH–H$_\beta$ relay cross-peaks of 13 mM octanoyl-ACP in 35 mM KH_2PO_4, pH 6.35, in H_2O/D_2O (4:1). The NH–H$_\alpha$ fingerprint cross-peaks appear at $\omega_1 > 3.2$ ppm, and most of the NH–H$_\beta$ relay cross-peaks appear at $\omega_1 < 3.2$ ppm. The NH–H$_\alpha$ fingerprint, and NH–H$_\beta$ relay "(r)" cross-peaks for the alanines and threonines are labeled. The presence of an NH–H$_\beta$ relay cross-peak for T64 is indicated because it is evident upon plotting at a lower contour level.

Identification of Spin Systems. Since we will rely on amide resonances to place amino acids in sequence, it makes sense to focus our identification efforts in a region that shows the connection of amide proton resonances to resonances that are more characteristic of amino acid type. A useful region in this respect is the fingerprint region of COSY spectra, where cross-peaks connecting the amide and α-proton resonances appear. While useful, α-proton resonances often exhibit severe overlap, limiting the ultimate utility of the fingerprint region. In contrast, β-proton resonances are less prone to overlap, often allowing one to bypass crowded portions of the fingerprint. Relayed COSY spectra contain both NH–H$_\alpha$ and NH–H$_\beta$ connectivities. Figure 1 shows a portion of an octanoyl-ACP relayed COSY data set, where NH–H$_\alpha$ fingerprint ($\omega_1 \sim$ 5.2–3.2 ppm) and NH–H$_\beta$ relay ($\omega_1 \sim <3.2$ ppm) cross-peaks appear. While most of the NH–H$_\beta$ relay cross-peaks lie well outside the fingerprint region, there are a few that appear

inside. In general, these cross-peaks are for amino acids with β-proton resonances far downfield and are easily distinguished from fingerprint cross-peaks by comparing COSY and relayed COSY spectra. Examples of such cross-peaks are the threonine NH–H_β relay cross-peaks [indicated by an "(r)" designation in Figure 1]. In contrast, the alanine NH–H_β relay cross-peaks [also indicated by an "(r)" designation] appear in a region more usually associated with NH–H_β relay cross-peaks.

A good example of how relayed COSY data supplements COSY data is found in the way in which the alanine and threonine spin systems were identified for octanoyl-ACP. COSY data acquired in D_2O indicated 13 low-field methyl resonances that could be either alanine β-CH_3's or threonine γ-CH_3's. Both alanine and threonine have methyls that give rise to COSY cross-peaks in the same area. In principle, one can distinguish alanine from threonine by observation of a second COSY cross-peak connecting a threonine β-CH to a threonine α-CH resonance. In practice, such cross-peaks were clearly resolved in only two cases. In the relayed COSY spectrum, strong NH–β-CH_3 relay cross-peaks, which are characteristic of alanine, were found in a well-resolved, distinctive region, allowing identification of all seven alanines in octanoyl-ACP. NH–β-CH relay cross-peaks characteristic of threonine were also found in four cases, and a α-CH–γ-CH_3 relay cross-peak allowed partial identification of a fifth threonine. The sixth threonine was not found at this point.

In addition to the alanines and threonines, the combined use of COSY and relayed COSY data permitted the identification of the complete coupled spin systems for four out of the four glycines present in octanoyl-ACP and seven out of seven of the valines. Six out of seven isoleucine NH–H_α–H_β–γ-CH_3 fragments were found. Thirteen AMXY (NH–H_α–β-CH_2) spin systems were also identified, from which the complete spin systems corresponding to the two phenylalanines, the tyrosine, and the histidine were identified with aromatic ring proton–β-CH_2 NOEs (Billeter et al., 1982). Furthermore, 29 long side chain spin systems (NH–H_α–β-CH_2–X fragments) were found. The use of the relayed COSY data allowed identification of at least one of the two β-proton resonances for each of these spin systems. In turn, this allowed the conditional identification of four lysines in octanoyl-ACP, on the basis of the distinctive appearance of the α–β cross-peaks (Weber et al., 1985b).

Sequential Assignment of Spin Systems. The rationale behind most sequential assignment processes is straightforward: connect as many previously identified residues as possible together until a unique sequence is found. A good example of how the sequential assignment process was carried out for octanoyl-ACP is offered by the assignment of the segment from A59 to A68. The reasons for choosing this segment as an illustration are twofold: (1) The sequence from E60 to T64 was one of the more difficult sequences to assign in ACPSH, and in comparison to the relatively straightforward strategy presented here, it illustrates how minor changes in resonance positions can ease assignment problems. (2) When we compare chemical shifts of residues in ACPSH and octanoyl-ACP, we will find this to be one of the regions of major differences. Thus, confidence in our assignments of this region is essential.

On examination of the amino acid sequence, it was found that the -T63-T64- segment was unique, and since the amides for all the threonines except two had been identified, it was felt that looking for a -T-T- connectivity as a starting point was justified. Examination of the NOESY spectrum revealed the presence of a d_{NN} cross-peak connecting the amides of two spin systems previously assigned to threonine on the basis of COSY and relayed COSY spectra. The sequential relationship of these two residues was confirmed by the presence of both $d_{\alpha N}$ and $d_{\beta N}$ cross-peaks connecting the same spin systems. Moreover, the directional characteristics of $d_{\alpha N}$ and $d_{\beta N}$ cross-peaks [NH(i)–H$_\alpha$(i – 1) cross-peaks are seen, while NH(i)–H$_\alpha$(i + 1) are not] revealed which threonine was T63 and which was T64. Once a unique starting point had been found, all that remained was to connect residues to this point and verify that they matched sequence predictions. Only one other cross-peak was found to connect to the T63 amide resonance. That cross-peak was a $d_{\alpha N}$ cross-peak to an isoleucine. Since this connection could not be verified with other cross-peaks and since $d_{\alpha N}$ cross-peaks are known to occur occasionally for nonsequential residues (Billeter et al., 1982), the assignment of the isoleucine as I62 remained conditional at this point. The putative I62, however, showed a clear d_{NN} connection to the amide of a spin system conditionally identified as a lysine, which would be consistent with the sequence -K-I-. The presumed K61 was found to have a d_{NN} cross-peak to the amide of a long side chain spin system, which in turn had d_{NN}, $d_{\alpha N}$, and $d_{\beta N}$ cross-peaks to an alanine. Assuming that d_{NN} cross-peaks represent only sequential connectivities, this led to -A-X-K-I-. Even if we assumed that our conditional identification of the lysine was wrong, the segment -A-X-X-I- is unique only to one position: -A59-E60-K61-I62-. Moreover, the assignment of E60 is consistent with its previous identification as a long side chain spin system.

In the other direction, a $d_{\alpha N}$ connectivity linked a valine amide, presumably V65, with T64. A d_{NN} and a $d_{\beta N}$ connectivity connected a long side chain amino acid to the putative V65. A d_{NN} and a $d_{\alpha N}$ connectivity attached an alanine to this long side chain residue, while a d_{NN} and a $d_{\beta N}$ connectivity linked a second alanine to the first. There is only one instance of -A-A- in ACP, so this segment is consistent with -V65-Q66-A67-A68-. Thus, we have a complete assignment for the segment from A59 to A68.

A similar process led to most of the assignments in octanoyl-ACP. The predictions of a high α-helical content for octanoyl-ACP were borne out in the sequential assignment step: 88% of all the residues were assigned on the basis of d_{NN} connectivities. A further 4% were assigned primarily on the basis of $d_{\alpha N}$ connectivities, most notably T3, T23, and S27. Residues D38 and I54 merit special comment. Residue D38 is not assigned because we are missing a fingerprint cross-peak assignable to aspartic acid. A very weak irregularity in the relayed COSY fingerprint region appears about where comparison with ACPSH data suggests that a D38 fingerprint might appear, but this is not strong enough to constitute an assignment. A similar situation occurs with I54. However, if the relayed COSY spectrum is processed to maximize signal at the expense of resolution, a weak NH–H_α fingerprint and a NH–H_β relay cross-peak become evident in a region appropriate for an isoleucine. Although there are no cross-peaks in the NOESY spectrum to allow sequential assignment, the J-coupling pattern of this spin system is very characteristic of isoleucine. Since I54 and D38 were at this point the only unassigned residues in octanoyl-ACP, this spin system is assigned to I54.

An overview of α- and amide proton resonance assignments for octanoyl-ACP is presented in Figure 2, as a pseudo-two-dimensional map of the fingerprint region, with the corresponding ACPSH data included for comparison. In this figure, dotted lines indicate the positions of fingerprint cross-peaks that differ the most between the two species. In addition, a

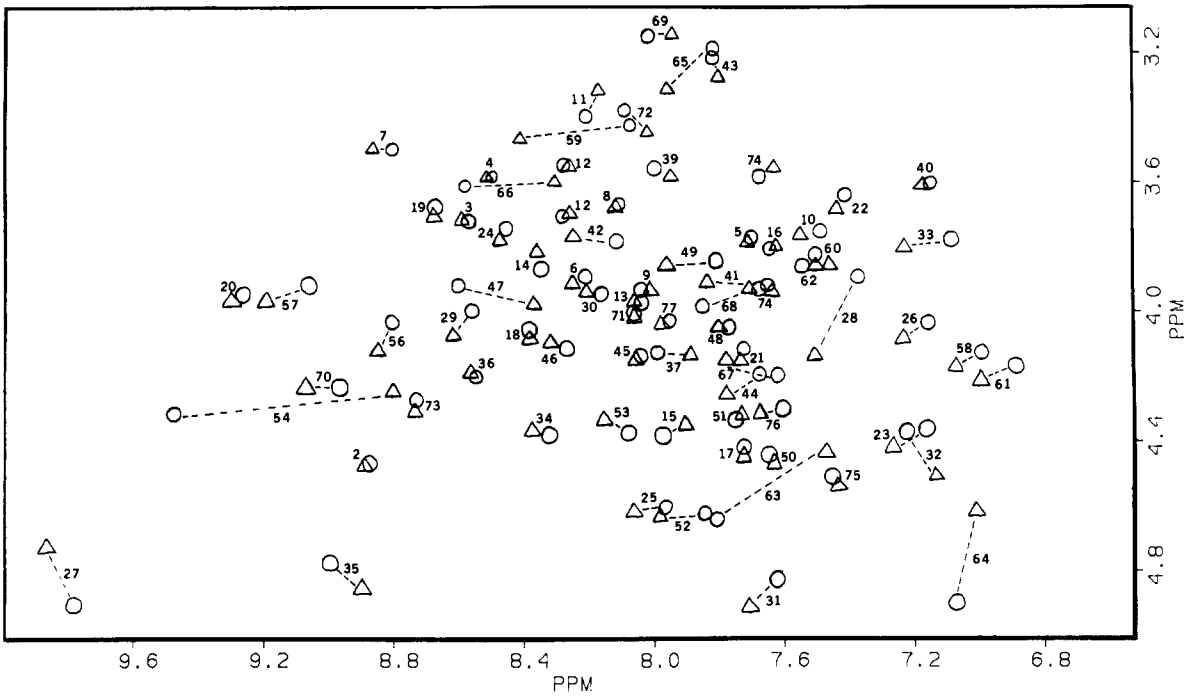

FIGURE 2: Pseudo-two-dimensional map comparing octanoyl-ACP (○) and ACPSH (△) NH–H_α fingerprint cross-peak positions. Dotted lines indicate the residues for which the change is greatest. Experimental conditions: octanoyl-ACP/ACPSH: 13/10 mM in 35/55 mM KH_2PO_4 at pH 6.35/5.6. Both spectra were recorded at 303 K in H_2O/D_2O (4:1).

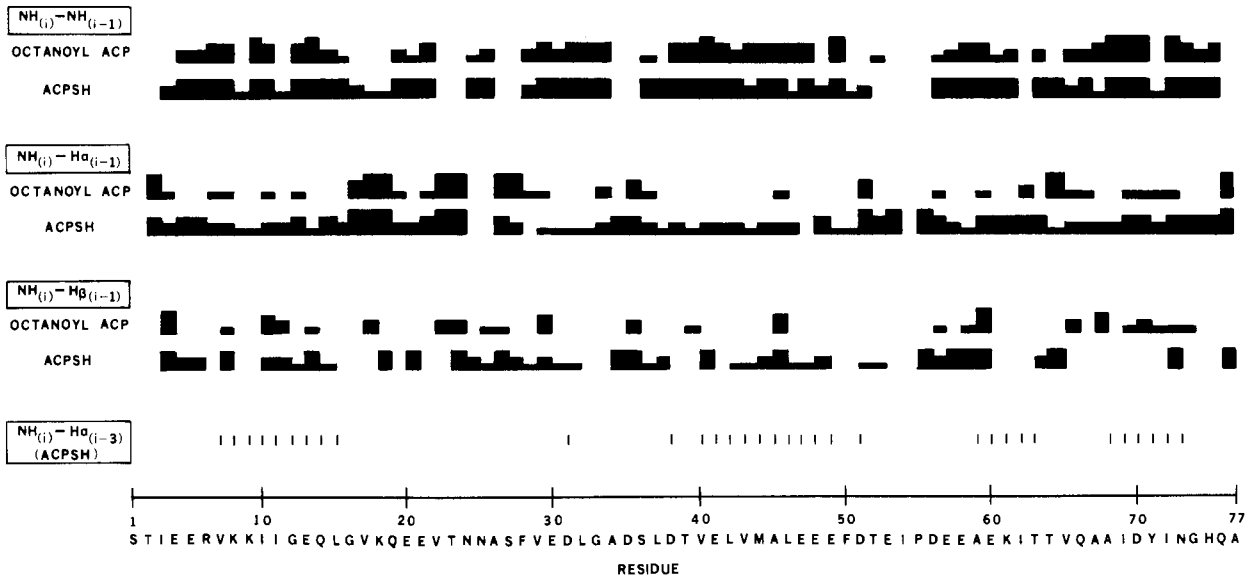

FIGURE 3: Comparison of sequential NOE connectivities observed for octanoyl-ACP and ACPSH. The NOEs are classified as weak, medium, strong, and very strong and are represented by bars indicating the sequential positions connected by a particular NOE. The height of the bar reflects the NOE's intensity classification. In addition, long-range connectivities observed in ACPSH, which are characteristic of α-helices, are shown at the appropriate NH position. The data on octanoyl-ACP/ACPSH was acquired from a 15/10 mM sample in 35/250 mM KH_2PO_4, pH 6.5/5.6, with a mixing time of 160/180 ms.

summary of the distribution and intensity of the NOESY cross-peaks used in obtaining the assignments for octanoyl-ACP and ACPSH is presented in Figure 3, where the intensity of the observed cross-peaks is reflected in the height of the bars representing the cross-peaks.

Discussion

In large part, the assignment of octanoyl-ACP resonances yielded chemical shifts analogous to those for corresponding resonances in ACPSH. This is evident by comparing the fingerprint regions of octanoyl-ACP and ACPSH, as presented in Figure 2. While many of the cross-peaks show a close position homology, there are a number that have quite different positions in the two species. Even with these nearly identical molecules, it now becomes clear that it would not have been possible to get assignments solely on the basis of cross-peak position homologies with ACPSH.

It is difficult to be definitive about the origins of changes in chemical shift. Most are too small to be signficant and probably are consistent with a model where the introduction of a fatty acid causes minor structural rearrangement but preserves the overall secondary structural characteristics of ACPSH. The larger shifts can arise from either direct effects due to the proximity of the acyl chain or local conformational changes induced by its presence. Not all resonances respond equally to both factors. For example, the chemical shifts of

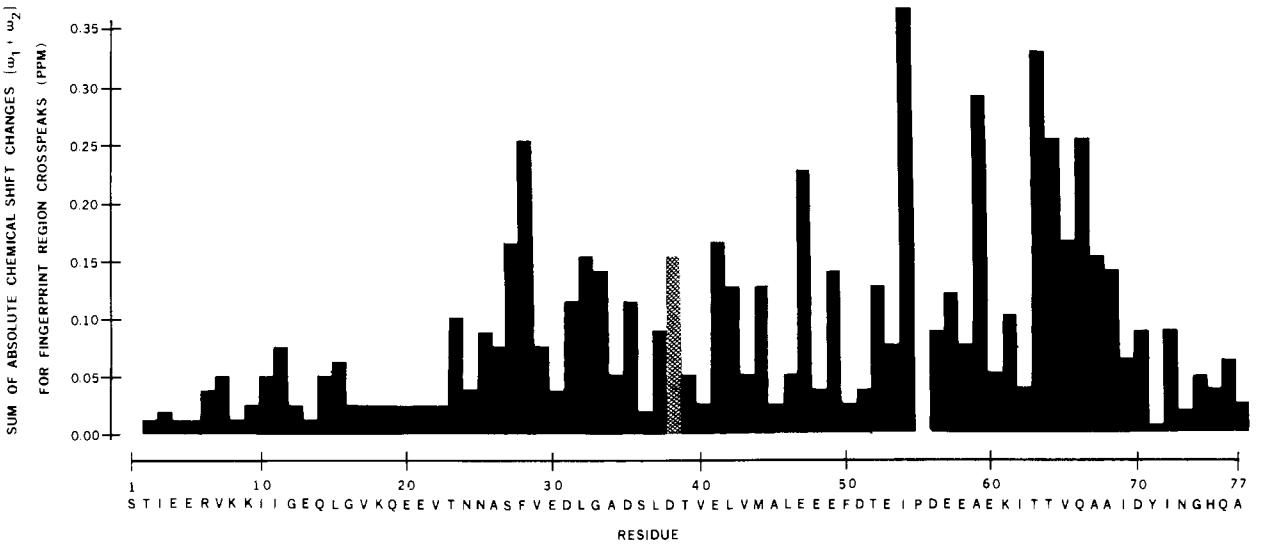

FIGURE 4: Sum of the absolute magnitudes of chemical shift changes in the ω_1 and ω_2 dimensions between octanoyl-ACP and ACPSH NH–H_α fingerprint cross-peaks, plotted against residue number. The data for D38 is tentative, as a firm assignment of the NH–H_α fingerprint cross-peak of D38 in octanoyl-ACP is not available at this time (see text).

amide protons are very sensitive to hydrogen bonding and solvent exposure, while α-proton chemical shifts are less sensitive. Since perturbations in hydrogen-bonding networks and changes in solvent exposure are often directly associated with small conformational changes, such changes are more likely to produce a difference in the chemical shift of an amide proton than the corresponding α-proton. Thus, if a fingerprint cross-peak shifts primarily in the amide dimension, conformational changes in the protein are to be suspected. Moreover, since conformational changes tend to affect regions of a protein, such effects would probably be less localized than the effects from the proximity of an acyl chain. Inspection of Figure 2 reveals that the fingerprint cross-peak movements tend to be predominantly in the amide dimension and are spread over many residues in the protein. An observation such as this is consistent with the presence of the fatty acid inducing minor structural changes in ACP.

Any localization of structural changes to certain regions of the protein is certainly of interest. In order to more easily recognize such localized change, the sum of the absolute value of the changes in chemical shift, in both the amide and the H_α dimensions for the fingerprint cross-peaks, is plotted against residue number in Figure 4. On inspection of this figure, it is apparent that changes are widely spread, with no apparent pattern except for two regions. First, fingerprint cross-peak shifts for residues 1–20 are relatively small and appear to have a regular periodicity. By inspection, this periodicity appears to be governed by a four-residue repeat. This conclusion is verified by plotting the correlation function for the cross-peak shifts of the first 20 residues, as presented in Figure 5A. Second, there is a consistently large change in cross-peak positions seen for residues 63–69. This, as well as the shifts for the rest of the cross-peaks between residues 20–77, shows no obvious periodicities. The lack of obvious peaks in the correlation function presented in Figure 5B confirms the lack of periodicities in the cross-peak shifts for residues 20–77.

In order to better understand these cross-peak shifts in the context of any changes in secondary structure on interaction of the fatty acid with the protein, a more direct comparison of octanoyl-ACP and ACPSH secondary structures is in order. Inferences about protein secondary structure from the type and intensity of interresidue cross-peaks seen in NOESY spectra have been made in the case of several proteins. It has

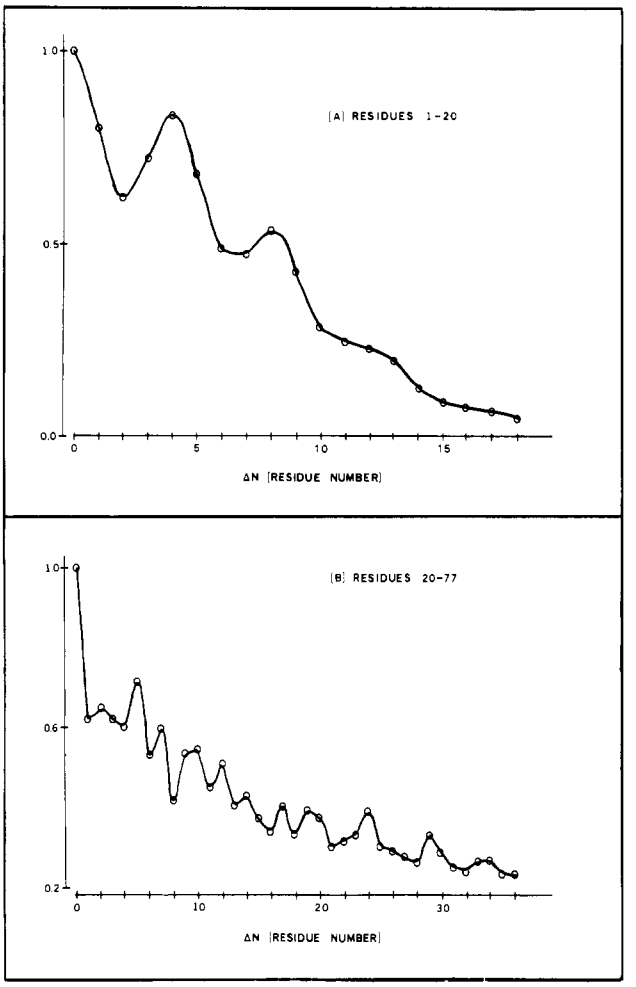

FIGURE 5: Plot of the correlation function of NH–H_α fingerprint cross-peak shifts between octanoyl-ACP and ACPSH as a function of residue number for residues 1–20 (A) and 20–77 (B).

been found that regions of extended conformation are characterized by strong $d_{\alpha N}$ connectivities and that β-turns give rise to isolated occurrences of strong $d_{\alpha N}$ and/or d_{NN} connectivities. In addition to the strong d_{NN} and $d_{\beta N}$ connectivities mentioned earlier, α-helices are also characterized by NH(i)–$H_\alpha(i-3)$ and NH(i)–$H_\alpha(i-4)$ connectivities (Billeter et

al., 1982; Wuthrich et al., 1984). Unfortunately, the spectral quality of the NOESY data acquired from octanoyl-ACP is not sufficiently high to permit detection of many of these longer range connectivities, although those that are detected are consistent with what is observed for ACPSH. However, when the intensities of the d_{NN}, $d_{\alpha N}$, and $d_{\beta N}$ cross-peaks present in octanoyl-ACP NOESY spectra are plotted alongside the corresponding ACPSH data as presented in Figure 3, it becomes evident that there is a moderately high degree of homology in the connectivities seen in the two species. This is particularly apparent for the NH–NH cross-peaks. In the NH–H_α and NH–H_β comparisons, the cross-peaks observed for octanoyl-ACP are, in general, strong cross-peaks in ACPSH. The absence of cross-peaks in octanoyl-ACP, which are weak in ACPSH, is not necessarily meaningful because they could be lost because of the lower signal levels in the octanoyl-ACP spectra. On this basis, it is reasonable to assume that the secondary structures of the two proteins are quite similar, if not identical.

There is however, one exception to this general rule. In octanoyl-ACP, from residue V65 to residue Y71, there is a set of moderately strong $d_{\beta N}$ cross-peaks where none were observed in ACPSH. In addition, there is a considerable difference in the intensity seen for the $d_{\alpha N}$ cross-peak connecting T63 and V64 and the intensity distribution for the d_{NN} cross-peaks involving residue T64 to residue A69. Although the reasons for these departures are unclear, it is interesting to note that this is nearly the same portion of the protein where the fingerprint cross-peaks in octanoyl-ACP exhibit consistently large shifts compared with those of ACPSH. The secondary structural analysis of this region in ACPSH implied that it is a connecting segment between two short helices. A model consistent with these observations is that this short segment acts as a hinge connecting the two helices which opens (or closes) to accommodate the fatty acid. Such a conformational change is consistent with the observation that many of the cross-peak shifts for these residues are primarily shifts in the amide dimension.

On considering secondary structure, a straightfoward interpretation of the periodicity seen in the cross-peak shifts for the first 20 residues emerges. Since the N-terminal helix was found to exist from residue 3 to residue 15 and since the four-residue repeat seen is consistent with the pitch of an α-helix, an obvious explanation is that the introduction of the fatty acid produces a change that affects only one side of the helix. Since terminal helices tend to be less constrained than internal ones, the most plausible change would be a small movement of the intact N-terminal helix. It is unlikely that such a movement results from the proximity of the acyl chain, as the cross-peak shifts for these residues are among the smallest observed.

Additional evidence in favor of a small tertiary structural rearrangement of the protein on the introduction of a fatty acid comes from the observation that there are a few differences in the set of long-range NOE contacts seen for octanoyl-ACP and ACPSH. While the interpretation of these changes will not be possible until the tertiary structure of the protein is more well defined, the fact that such changes are observed indicates that the structural rearrangement may be more than just a rearrangement of side chains.

Thus, the data for octanoyl-ACP is consistent with a general preservation of secondary structural elements, with the largest alteration being a change in the region connecting the two carboxyl-terminal helices. The identification of conserved structural elements and areas of structural rearrangement is a step toward a description of the manner in which fatty acids modulate the structure of ACP and a step toward understanding its function in fatty acid synthesis.

ACKNOWLEDGMENTS

We thank P. Demou for assisting with the instrumental aspects of this work.

REFERENCES

Aue, W. P., Bartholdi, E., & Ernst, R. R. (1976) *J. Chem. Phys. 64*, 2229–2246.
Barnes, E. M., & Wakil, S. J. (1968) *J. Biol. Chem. 243*, 2955–2962.
Bax, A., & Freeman, R. (1981) *J. Magn. Reson. 44*, 542–561.
Bax, A., & Drobny, G. (1985) *J. Magn. Reson. 61*, 306–320.
Billeter, M., Braun, W., & Wuthrich, K. (1982) *J. Mol. Biol. 155*, 321–346.
Cronan, J. E., Jr., & Klages, A. L. (1981) *Proc. Natl. Acad. Sci. U.S.A. 78*, 5440–5444.
Eich, G., Bodenhausen, G., & Ernst, R. R. (1982) *J. Am. Chem. Soc. 104*, 3731–3732.
Holak, T. A., & Prestegard, J. H. (1986) *Biochemistry 25*, 5766–5774.
Ikura, M., Minowa, O., & Hikichi, K. (1985) *Biochemistry 24*, 4264–4269.
Klevit, R. E., & Waygood, E. B. (1986) *Biochemistry 25*, 7774–7781.
Klevit, R. E., Drobny, G. P., & Waygood, E. B. (1986) *Biochemistry 25*, 7760–7769.
Kumar, A., Ernst, R. R., & Wuthrich, K. (1980) *Biochem. Biophys. Res. Commun. 95*, 1–6.
Macura, S., & Ernst, R. R. (1980) *Mol. Phys. 41*, 95–117.
Majerus, P. W., Alberts, A. W., & Vagelos, P. R. (1965) *J. Biol. Chem. 240*, 4723–4726.
Mayo, K. H., Tyrell, P. M., & Prestegard, J. H. (1983) *Biochemistry 22*, 4485–4493.
McRee, D. E., Richardson, J. S., & Richardson, D. C. (1985) *J. Mol. Biol. 182*, 467–468.
Neuhaus, D., Wagner, G., Vasak, M., Kagi, J. H. R., & Wuthrich, K. (1985) *Eur. J. Biochem. 151*, 257–273.
Pugh, E. L., & Wakil, S. J. (1965) *J. Biol. Chem. 240*, 4727–4733.
Rock, C. O., & Cronan, J. E., Jr. (1979) *J. Biol. Chem. 254*, 9778–9785.
Rock, C. O., & Garwin, J. L. (1979) *J. Biol. Chem. 254*, 7123–7128.
Rock, C. O., & Cronan, J. E., Jr. (1980) *Anal. Biochem. 102*, 362–364.
Schulz, H. (1975) *J. Biol. Chem. 250*, 2299–2304.
Spencer, A. K., Greenspan, A. D., & Cronan, J. E., Jr. (1978) *J. Biol. Chem. 253*, 5922–5926.
Strop, P., Wider, G., & Wuthrich, K. (1983) *J. Mol Biol. 166*, 641–667.
Takagi, T., & Tanford, C. (1968) *J. Biol. Chem. 243*, 6432–6435.
Therisod, H., Weissborn, A. C., & Kennedy, E. P. (1986) *Proc. Natl. Acad. Sci. U.S.A. 83*, 7236–7240.
Vagelos, P. R. (1973) *Enzymes (3rd Ed.) 8*, 155–199.
Vanaman, T. C., Wakil, S. J., & Hill, R. L. (1968a) *J. Biol. Chem. 243*, 6409–6419.
Vanaman, T. C., Wakil, S. J., & Hill, R. L. (1968b) *J. Biol. Chem. 243*, 6420–6431.
Volpe, J. J., & Vagelos, P. R. (1976) *Physiol. Rev. 56*, 339–417.
Wagner, G., & Wuthrich, K. (1982) *J. Mol. Biol. 155*, 347–366.

Weber, P. L., Drobny, G., & Reid, B. R. (1985a) *Biochemistry 24*, 4549–4552.
Weber, P. L., Wemmer, D. E., & Reid, B. R. (1985b) *Biochemistry 24*, 4553–4562.
Wemmer, D. E., Kumar, N. V., Metrione, R. M., Lazdunski, M., Drobny, G., & Kallenbach, N. R. (1986) *Biochemistry 25*, 6842–6849.
Wider, G., Macura, S., Kumar, A., Ernst, R. R., & Wuthrich, K. (1984) *J. Magn. Reson. 56*, 207–234.
Williamson, M. P., Marion, D., & Wuthrich, K. (1984) *J. Mol. Biol. 173*, 341–359.
Wuthrich, K. (1983) *Biopolymers 22*, 131–138.
Wuthrich, K., Billeter, M., & Braun, W. (1984) *J. Mol. Biol. 180*, 715–740.
Zuiderweg, E. R. P., Kaptein, R., & Wuthrich, K. (1983a) *Eur. J. Biochem. 137*, 279–292.
Zuiderweg, E. R. P., Kaptein, R., & Wuthrich, K. (1983b) *Proc. Natl. Acad. Sci. U.S.A. 80*, 5837–5841.

Locus of a Histidine-Based, Stable Trifunctional, Helix to Helix Collagen Cross-Link: Stereospecific Collagen Structure of Type I Skin Fibrils†

Gerald L. Mechanic,* Elton P. Katz,‡ Masayuki Henmi,§ Claudia Noyes,‖ and Mitsuo Yamauchi

Dental Research Center and Department of Biochemistry and Nutrition, University of North Carolina at Chapel Hill, Chapel Hill, North Carolina 27514, and University of Connecticut Health Center, Farmington, Connecticut 06032

Received June 30, 1986; Revised Manuscript Received January 29, 1987

ABSTRACT: The loci of the three amino acid residues that contribute their prosthetic groups to form the stable, nonreducible, trifunctional intermolecular cross-link histidinohydroxylysinonorleucine in skin collagen fibrils were identified. Two apparently homogeneous three-chained histidinohydroxylysinonorleucine cross-linked peptides were chromatographically isolated. They were obtained from a tryptic digest of denatured unreduced 6 M guanidine hydrochloride insoluble bovine skin collagen. Amino acid and sequence analyses demonstrated that the prosthetic groups of α1(I)-chain Hyl-87, α1(I)-chain Lys-16^c, and α2(I)-chain His-92 formed the cross-link. The latter results served to define the locus of the stable, nonreducible trifunctional moiety. Identical types of analyses were performed on the three-chained peptides isolated after bacterial collagenase digestion of the cross-linked tryptic peptides. This confirmed the initial identification and location of the three peptides linked by the cross-link. In addition, data reported here provide for a correction of the micromolecular structure for the α2(I) chain. Stereochemical considerations concerning this trifunctional cross-link's specific locus indicate that the steric relationships between the α chains of skin and skeletal tissue collagens are fundamentally different and the intermolecular relationships in skin fibrils are specific for skin. The same molecular relationships also indicate that histidinohydroxylysinonorleucine links three molecules of collagen. The stereochemistry of cross-linking for skin collagen is in accordance with and explains the X-ray findings of a 65-nm periodicity found for this tissue [Stinson, R. H., & Sweeny, P. R. (1980) *Biochim. Biophys. Acta 621*, 158; Brodsky, B., Eikenberry, E. F., & Cassidy, K. (1980) *Biochim. Biophys. Acta 621*, 162].

Covalent cross-links between collagen molecules, packed into fibrillar arrays, are principal determinants of the mechanical properties of connective tissue matrices. The cross-linking stereochemistry derives from the reaction of specific peptidyl aldehydes, in the NH_2- and COOH-terminal nonhelical peptides, with vicinal ϵ-amino groups of specific peptidyl residues of Lys and Hyl, located in the triple-helical regions of molecules (Yamauchi et al., 1986). His, a sparse amino acid (0.4 residue percent) in collagen, surprisingly also participates in cross-links (Tanzer et al., 1973; Housley et al., 1975; Bernstein & Mechanic, 1980). The cross-linking chemistry in type I collagen fibrils initially involves residues from two collagen chains, but subsequently, residues from other chains participate to form tri- and tetrachain cross-links. The initial cross-link at the COOH-terminal locus covalently ties together two α chains from different collagen molecules by means of an iminium bond (Fukae & Mechanic, 1980; Yamauchi et al., 1986). The reacting moieties are specifically dictated by the intermolecular stagger in the fibril, which juxtaposes the 5-amino-5-carboxypentanal (Lys^{ald})[1] or Hyl^{ald} residue, in the COOH-terminal nonhelical peptide position 16^c of an α1(I) chain, with the ϵ-amino of Hyl-87 in the helical region of either an α1(I) or α2(I) chain (Yamauchi et al., 1986). When residue 16^c is Hyl^{ald}, rearrangement of the iminium to a ke-

† This investigation was supported by National Institutes of Health Grants AM 19969, AM 30587, AM 37604, and DE 02668 and National Aeronautics and Space Agency Grant NAG 2-181.

* Author to whom correspondence should be addressed at the Dental Research Center.
‡ Present address: Department of Biostructure and Function, University of Connecticut Health Center, Farmington, CT 06032.
§ Present address: Tsurumi University, Tsurumi, Japan. Postdoctoral Fellow–Research Associate in the laboratory of G.L.M., 1984–1985.
‖ Present address: Department of Medicine, University of North Carolina at Chapel Hill, Chapel Hill, NC 27514.

[1] Abbreviations: deH-HHMD, dehydrohistidinohydroxymerodesmosine; HHL, histidinohydroxylysinonorleucine; Lys^{ald}, 5-amino-5-carboxypentanal; Hyl^{ald}, 2-hydroxy-5-amino-5-carboxypentanal; Gdn·HCl, guanidine hydrochloride; NEM, *N*-ethylmaleimide; TPCK, L-1-(tosylamido)-2-phenylethyl chloromethyl ketone; DEAE, diethylaminoethyl; Tris, tris(hydroxymethyl)aminomethane.

0006-2960/87/0426-3500$01.50/0